CHEMMEDCHEM

CHEMISTRY ENABLING DRUG DISCOVERY

Accepted Article

Title: Design, synthesis, biological evaluation, and X-ray studies of HIV-1 protease inhibitors with modified P2'-ligands of Darunavir

Authors: Arun K Ghosh, W. Sean Fyvie, Margherita Brindisi, Melinda Steffey, Johnson Agniswamy, Yuan-Fang Wang, Manabu Aoki, Masayuki Amano, Irene T. Weber, and Hiroaki Mitsuya

To be cited as: *ChemMedChem* 10.1002/cmdc.201700614

Link to VoR: http://dx.doi.org/10.1002/cmdc.201700614

A Journal of

ChemPubSoc Europe

WILEY-VCH

www.chemmedchem.org

WILEY-VCH

FULL PAPER

Design, synthesis, biological evaluation, and X-ray studies of HIV-1 protease inhibitors with modified P2'-ligands of Darunavir

Arun K. Ghosh*[a], W. Sean Fyvie,[a] Margherita Brindisi,[a] Melinda Steffey,[a] Johnson Agniswamy,[b] Yuan-Fang Wang,[b] Manabu Aoki,[c] Masayuki Amano,[c] Irene T. Weber,[b] and Hiroaki Mitsuya [c,d,e]

[a] Prof. Dr. A. K. Ghosh, Dr. W. Sean Fyvie, Dr. M. Brindisi, and Ms. M. Steffey
Department of Chemistry and Department of Medicinal Chemistry
Purdue University, West Lafayette, IN 47907
E-mail: akghosh@purdue.edu
[b] Prof. Dr. I. T. Weber, Dr. J. Agniswamy, Dr. Y.-F. Wang
Departments of Biology and Chemistry, Molecular Basis of Disease
Georgia State University, Atlanta, GA 30303
[c] Dr. H. Mitsuya, Dr. M. Aoki, Dr. M. Amano
Departments of Hematology and Infectious Diseases
Kumamoto University School of Medicine
Kumamoto 860-8556, Japan
[d] Dr. H. Mitsuya
Experimental Retrovirology Section, HIV and AIDS Malignancy
Branch, National Cancer Institute, Bethesda, MD 20892
[e] Dr. H. Mitsuya
Center for Clinical Sciences, National Center for Global Heath and Medicine
Shinjuku, Tokyo 162-8655, Japan

Supporting information for this article is given via a link at the end of the document

Abstract: The structure-based design, synthesis, and biological evaluation of a series of nonpeptidic HIV-1 protease inhibitors with rationally designed P2' ligands are described. The inhibitors are designed to enhance backbone binding interactions, particularly at the S2'-subsite. Synthesis of inhibitors was carried out efficiently. The stereochemistry of alcohol functionalities of the P2'-ligands was set by asymmetric reduction of the corresponding ketone using (*R,R*)- or (*S,S*)-Noyori's catalysts. A number of inhibitors displayed very potent enzyme inhibitory and antiviral activity. Inhibitors **3g** and **3h** showed an enzyme K_i of 27.9 and 49.7 pM and antiviral activity of 6.2 and 3.9 nM, respectively. These inhibitors also remained quite potent against darunavir-resistant HIV-1 variants. An X-ray structure of inhibitor **3g** in complex with HIV-1 protease revealed key interactions in the S2'-subsite.

Introduction

The arrival of HIV/AIDS in the early 1980s marked the onset of a global pandemic.[1,2] This led to intense worldwide research efforts in academic and pharmaceutical laboratories for treatment of HIV infection and AIDS.[3,4] Enormous research advances in the mid-1990s fundamentally changed the prognosis of HIV/AIDS treatment and management of the disease. The advent of combined antiretroviral therapy (cART), involving the use of HIV-1 protease inhibitors (PIs) and reverse transcriptase inhibitors drastically improved life expectancy and reduced HIV-related mortality of patients who have access to this treatment regimen.[5,6] Recent improvement of first line cART and declines in the price of treatment have prompted further accessibility of cART to developing countries.[7,8] Despite the great strides, there are serious limitations to current treatment regimens including cost, toxicity, patient compliance, side effects, and resistance. Perhaps, the most imposing limitation is the rapid rate at which the HIV generates viable drug-resistant mutants under selection pressure.[9,10] PIs are an integral part of

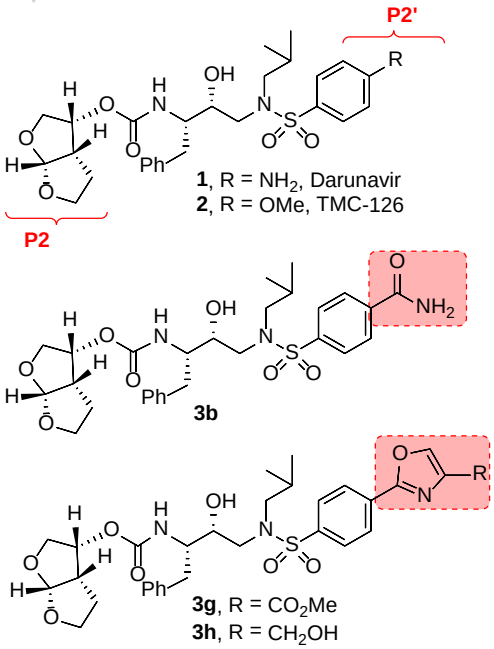

Figure 1. Structures of HIV-1 protease inhibitors **1** and **2** and of novel inhibitors **3b,g,h**.

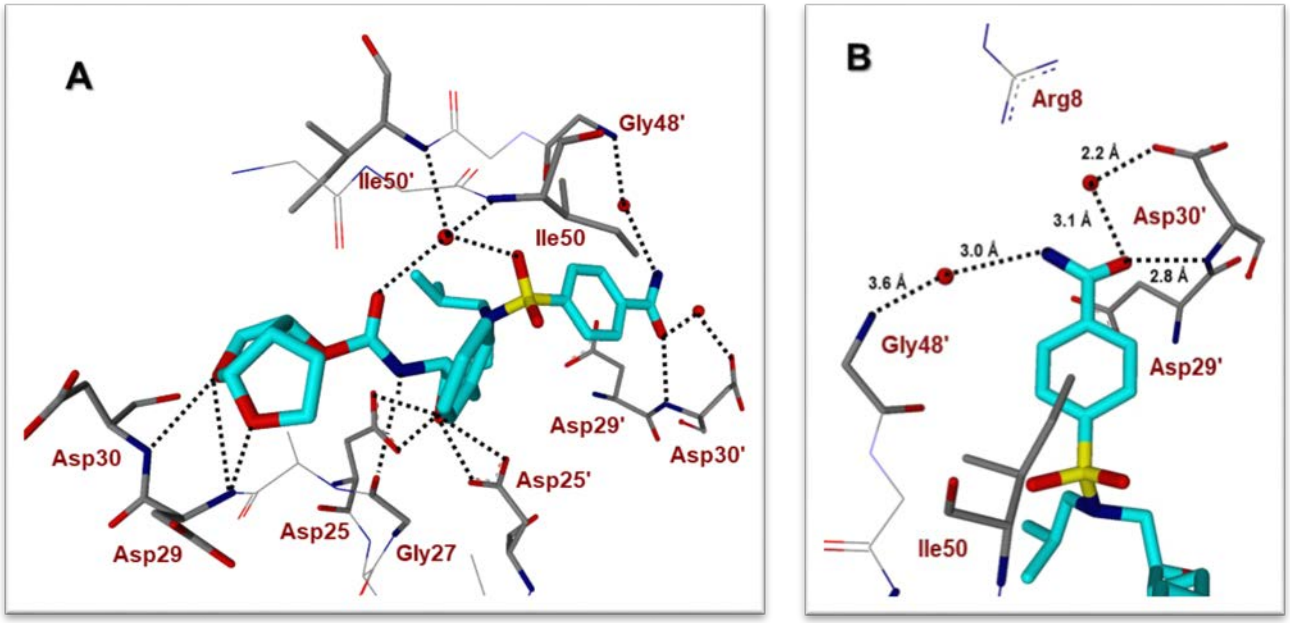

Figure 2. A. Inhibitor **3b**-bound X-ray structure of HIV-1 protease. The major orientation of the inhibitor is shown. The inhibitor carbon atoms are shown in turquoise, water molecules are red spheres, and the hydrogen bonds are indicated by dotted lines. **B.** Specific hydrogen bonding interactions of carboxamide are shown. These interactions are indicated with respective distances.

some of the most preferred cART treatment regimens.[11,12] In our continuing efforts to develop PIs to combat drug resistance, we designed several classes of novel compounds that displayed exceptional antiviral potencies across wild-type and multidrug-resistant HIV strains.[13,14] Inhibitor **1** (TMC-114 or Darunavir, DRV, Figure 1) displayed a picomolar enzyme inhibitory activity and very potent antiviral activity.[15,16] It was also endowed with unprecedented activity against a range of known multidrug resistant HIV strains.[17,18] Darunavir received FDA approval in 2006 for use in adult patients harboring drug-resistant strains.[15,16] In 2008, it was approved for all HIV/AIDS patients and emerged as a front line anti-HIV therapy for use in adult and pediatric patients.[19]

Our X-ray structural analysis of DRV-bound HIV-1 protease structure revealed an extensive network of hydrogen bonding interactions between DRV and backbone atoms of HIV-1 protease.[20] In particular, the *bis*-THF P2 ligand formed a pair of strong hydrogen bonds with Asp29 and Asp30 NHs in the S2-subsite. The P2'-aminosulfonamide forms a pair of hydrogen bonds with Asp30' backbone amide NH as well as with the Asp30' backbone carbonyl oxygen. These backbone interactions have been attributed to DRV's wide range of activity against known PI-resistant mutants.[15,21] The *bis*-THF ligands is a privileged ligand for DRV and its extensive interactions are responsible for DRV's unique activity. Over the years, we have investigated other structurally intriguing ligands that mimic the ligand-binding interactions of the *bis*-THF ligand of DRV in the S2 subsite. In an effort to promote further ligand-binding site interactions in the S2'-subsite, we have explored modifications of P2'-ligand with hydrogen-bonding donor/acceptor groups to form enhanced backbone interactions. We are particularly interested in ligands and scaffolds that may improve metabolic stability. In a preliminary effort, based upon the X-ray structure of DRV and HIV-1 complex, we incorporated a carboxylic acid and carboxamide functionalities at the 4-position of benzene ring of the P2'-sulfonamide ligand.[22,23] Both the carboxylic acid and the carboxamide ligand showed very potent low picomolar enzyme inhibitory activity. The carboxamide ligand derived inhibitor **3b** showed potent antiviral activity. To obtain ligand-binding site interactions of the carboxamide derivative, we determined an X-ray structure of **3b**-bound HIV-1 protease.[23] The key inhibitor-binding site interactions are shown in Figure 2A. In particular, the P2' moiety of **3b**, similarly to DRV, shows H-bond interactions with the backbone of Asp30'. Interestingly, the P2' benzene carboxamide moiety of **3b** also showed a conserved water-mediated bridging H-bond with Gly48' (Figure 2B).[24] Based upon this structure, we have now further modified P2'-ligand to promote hydrogen bonding interactions and improve antiviral activity using a range of stereochemically defined functionalities and heterocyclic scaffolds. Herein, we report the structure-based design, synthesis, X-ray structural studies and biological investigation of a series of HIV-1 PIs with novel P2'-ligands.

Synthesis of ligands and inhibitors

All target PIs herein presented are accessible via diacetate intermediate **5**, which has been prepared in two steps from commercially available chiral epoxide **4** as described previously.[25] The synthesis of compounds **3a-f** is reported in **Scheme 1**. Deprotection of **5** to the corresponding aldehyde with potassium carbonate in methanol and subsequent Pinnick oxidation led the carboxylic acid key intermediate **7** in excellent yield. Compound **7** was treated with trifluoroacetic acid (TFA) to remove the Boc group and the resulting TFA salt was treated with the known *bis*-THF activated carbonate **6**[26] in a 10/1 mixture of acetonitrile/water in the presence of *N*,*N*-DIPEA to provide inhibitor **3a**. Carboxamide inhibitor **3b** was prepared via direct

one-pot conversion of inhibitor **3a** to a mixed anhydride with di-*tert*-butyldicarbonate in the presence of pyridine followed by condensation with ammonium carbonate in 76% yield.[27]

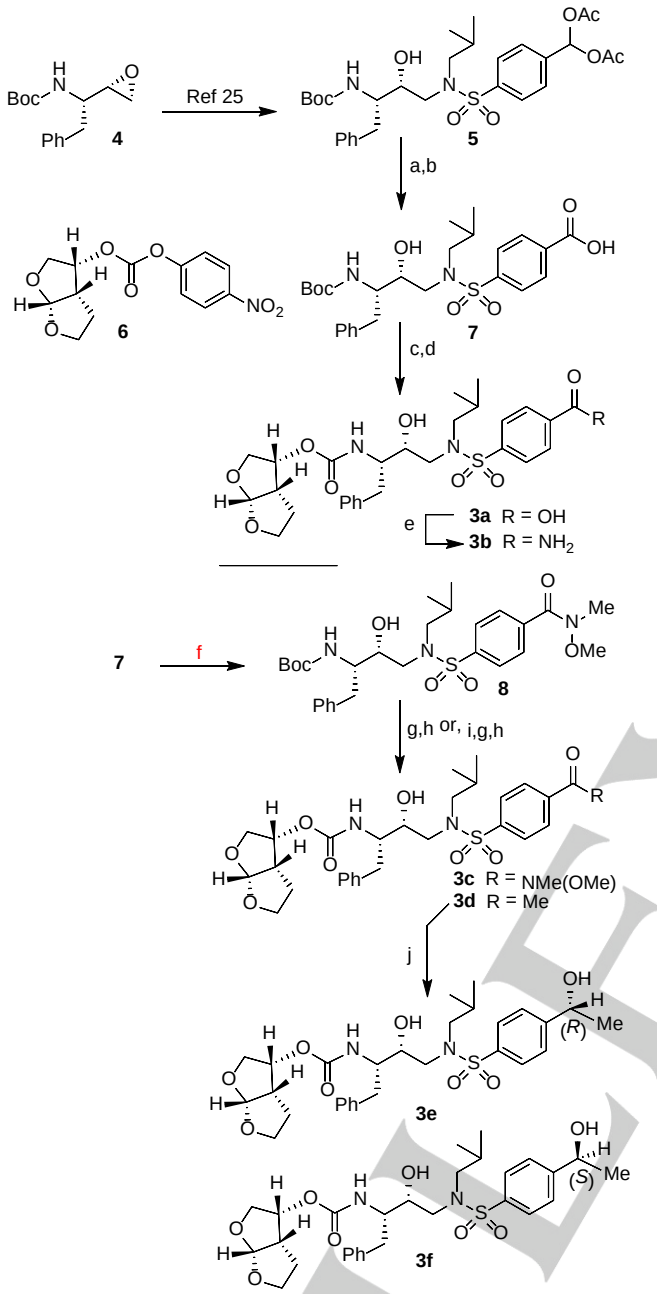

Scheme 1. Reagents and conditions: (a) K_2CO_3, MeOH, 23 °C, 1 h, 98%; (b) $NaClO_2$, *cis*-2-methyl-2-butene, $NaH_2PO_4 \cdot H_2O$, *t*-BuOH-H_2O, 23 °C, 50 min, 95%; (c) TFA, CH_2Cl_2, 23 °C, 3 h; (d) **6**, *N,N*-DIPEA, MeCN/H_2O, 23 °C, 3 days 89% (over 2 steps); (e) pyridine, Boc_2O, $(NH_4)_2CO_3$, THF, 23 °C, 14 h, 76%; (f) *i*BuOCOCl, NMM then MeNHOMe·HCl, dry CH_2Cl_2, -15 °C to 23 °C, 12 h, 76%; (g) TFA, CH_2Cl_2, 23 °C, 2 h; (h) **6**, *N,N*-DIPEA, MeCN, 23 °C, 5 days 73-78%; (i) MeMgBr (3M in Et_2O), dry THF, -78 °C, 4 h, 98%; (j) RuCl[(*R,R*)-TsDPEN](mesitylene) for **3e** or RuCl(*p*-cymene)[(*S,S*)-Ts-DPEN] for **3f**, TEA, HCOOH, dry CH_2Cl_2, 0 °C to 23 °C, 7 h, 94-98%.

Treatment of acid **7** with isobutyl chloroformate in the presence of *N*-methylmorpholine, followed by *N,O*-dimethylhydroxylamine led to the corresponding Weinreb amide **8**. Exposure to TFA followed by treatment with activated carbonate **6** and *N,N*-DIPEA in acetonitrile led to inhibitor **3c**. Intermediate **8** was also converted into its methyl ketone derivative by exposure to methylmagnesium bromide in dry THF. Boc deprotection followed by reaction with *bis*-THF derivative **6** led to final compound **3d**.

Inhibitors **3e,f** were prepared starting from compound **3d**. Exposure of **3d** to a catalytic amount (0.5 mol %) of the (*R,R*)- or (*S,S*)-Noyori's catalysts[28] in a 1:2 ratio of Et_3N/HCO_2H led to high yields (95-98%) of the corresponding (*R*) and (*S*) final alcohols **3e** and **3f**, respectively, with excellent enantioselectivity (see Experimental Section for HPLC analysis and details).

The synthesis of oxazole-containing inhibitors **3g,h** is reported in **Scheme 2**. Key carboxylic acid intermediate **7** was submitted to coupling reaction with serine methyl ester hydrochloride in the presence of EDCI, HOBt and *N,N*-DIPEA in dry DMF affording the corresponding amide adduct in 91% yield.

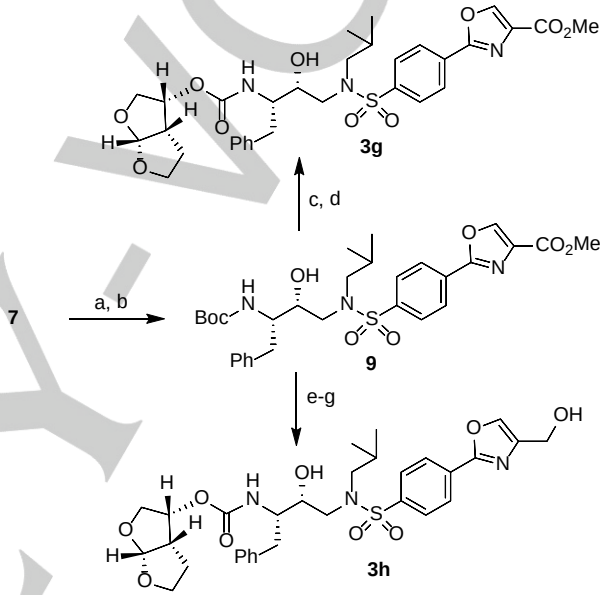

Scheme 2. Reagents and conditions: (a) DL-Serine methyl ester hydrochloride, EDCI, HOBt, *N,N*-DIPEA, dry DMF, 0 °C to 23 °C, 16 h, 91%; (b) DAST, dry CH_2Cl_2, - 78 °C, 30 min then $BrCCl_3$, DBU, dry CH_2Cl_2, 0 °C to 23 °C, 2.5 h, 64% (over 2 steps); (c) TFA, CH_2Cl_2, 23 °C, 4 h; (d) **6**, *N,N*-DIPEA, MeCN, 23 °C, 6 days, 61% (over 2 steps); (e) $NaBH_4$, EtOH, 0 °C to 23 °C, 24 h, 65%; (f) TFA, CH_2Cl_2, 23 °C, 4 h; (g) **6**, *N,N*-DIPEA, MeCN, 23 °C, 5 days, 60% (over 2 steps).

Subsequent dehydrative cyclization conditions with DAST reagent at -78 °C afforded the corresponding oxazoline intermediate immediately submitted to radical bromination-reductive elimination protocol using DBU/$BrCCl_3$ providing oxazole derivative **9** in 64% yield over 2 steps.[29] The reduction of the ester functionality of oxazole **9** with $NaBH_4$ in absolute ethanol provided the corresponding hydroxymethyl intermediate in moderate yield. Both the oxazole ester **9** and its hydroxymethyl derivative were converted to the corresponding final inhibitors **3g,h** via standard methods.

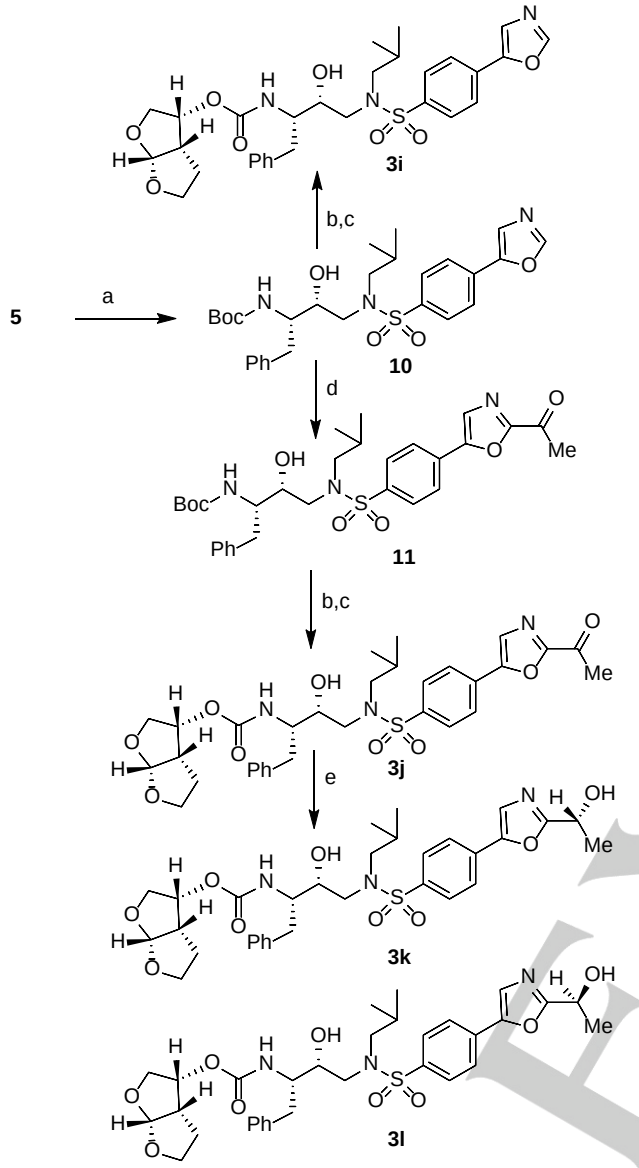

Scheme 3. Reagents and conditions: (a) TosMIC, K_2CO_3, MeOH, 55 °C, 1.5 h, 96%; (b) TFA, CH_2Cl_2, 23 °C, 2.5 h; (c) **6**, *N*,*N*-DIPEA, MeCN, 23 °C, 4-7 days, 47-80% (over 2 steps); (d) *i*PrMgCl, dry THF, -15 °C, 40 min then AcN(Me)OMe, -15 °C to 23 °C, 5 h, 79%; (e) RuCl[(*R*,*R*)-TsDPEN](mesitylene) for **3k** or RuCl(*p*-cymene)[(*S*,*S*)-Ts-DPEN] for **3l**, TEA, HCOOH, dry CH_2Cl_2, 0 °C to 23 °C, 7 h, 95-97%.

The second series of oxazole inhibitors **3i-l** was prepared as shown in **Scheme 3**. Diacetate intermediate **5** was converted to the oxazole derivative **10** in high yield employing the procedure reported by van Leusen and co-workers with toluenesulfonylmethyl isocyanide (TosMIC) in the presence of potassium carbonate in methanol.[30] Exposure of compound **10** to TFA followed by treatment with activated *bis*-THF derivative **6** in the presence of *N*,*N*-DIPEA led to inhibitor **3i**. Intermediate **10** was also treated with isopropylmagnesium chloride providing the 2-magnesiate derivative which was immediately reacted with the acetate-derived Weinreb amide to give the desired 2-acetyl oxazole **11** in good yield.[31] Acetyl derivative **11** underwent Boc-deprotection with TFA and treatment with activated *bis*-THF derivative **6** in the presence of *N*,*N*-DIPEA providing inhibitor **3j**. This latter also underwent Noyori's asymmetric hydrogenation with both the (*R*,*R*)- or (*S*,*S*)-Noyori's catalysts in a 1:2 ratio of Et_3N/HCO_2H leading to final compounds **3k,l** in high yields and enantiomeric excess (see Experimental Section for HPLC analysis and details).

Results and Discussion

We evaluated all synthetic inhibitors in HIV-1 protease inhibitory assay using the protocol developed by Toth and Marshall.[32] These results are shown in **Table 1**. Selected potent inhibitors were further evaluated in an antiviral assay following a reported protocol using MT-2 cells exposed to HIV-1_{LAI}.[33] In an attempt to promote hydrogen bond formation with the backbone atoms at S2' subsite, we investigated the feasibility of carboxylic acid, and various derivatives. As shown, incorporation of a *para*-carboxylic acid functionality provided inhibitor **3a** which showed very potent HIV-1 inhibitory activity (K_i = 12 pM). However, this carboxylic acid derivative showed antiviral IC_{50} value greater than 1 µM. Interestingly, the corresponding carboxamide derivative **3b** not only showed very potent HIV-1 protease inhibitory activity, but it also displayed potent antiviral activity (IC_{50} = 45 nM). The reason for poor antiviral activity for compound **3a** may be due to low cell penetration ability of carboxylic acids. Based upon the X-ray structure of DRV-bound HIV-1 protease, we speculated that carbonyl group of a carboxylic acid derivative or the heteroatoms of the corresponding heterocyclic derivatives can interact with backbone atoms particularly Asp29' and Asp30' backbone NHs. We therefore, investigated other carbonyl derivatives such as methoxymethyl amide in inhibitor **3c** as well as methyl ketone derivative in inhibitor **3d** (entries 3, 4). Interestingly, methyl ketone derivative **3d** displayed very potent enzyme K_i as well as antiviral activity. We have examined inhibitory properties of the corresponding reduction products, **3e** and **3f** (entries 5, 6). The stereochemical effect is apparent as compound **3e** with (*R*)-hydroxyl configuration has shown more than 4-fold improvement of enzyme K_i. Compound **3e** has shown potent antiviral IC_{50} of 4 nM.

We then pursued carboxylic acid bioisosteres with a series of oxazole-derived P2' ligands. As shown, compound **3g** and **3h**, bearing respectively a methyl ester and a hydroxymethyl functionality at the 4-position of the 2-phenyloxazole moiety, displayed a slight decrease of the enzyme inhibitory potency with K_i = 27.9 pM and K_i = 49.7 pM, respectively (entries 7 and 8). The corresponding reduction product alcohol **3h** displayed slightly improved antiviral IC_{50} value of 3.9 nM. We have also synthesized a series of carboxylic acid derivatives with 5-phenyloxazole scaffold (entries 9-12). These derivatives displayed reduction in enzyme inhibitory potency, however, they maintained excellent antiviral activity comparable to the activity of DRV. Monosubstituted derivative **3i** showed K_i of 126 pM and antiviral IC_{50} value of 2.8 nM (entry 9). Incorporation of methyl ketone at 2-position of the oxazole ring provided **3j**. This substitution did not improve potency and show activity similar to **3i** (entry 10). Reduction of methyl ketone provided stereochemically defined alcohols with (*R*)- and (*S*)-configuration. Both derivatives showed potent antiviral activity, however, no improvement was observed over monosubstituted oxazole derivative **3i** (entries **11** and **12**).

Table 1. Structures and activity of inhibitors **3a-l.**

Entry	Inhibitor structure	K_i[a] (pM)	IC_{50}[b,c] (nM)
1.	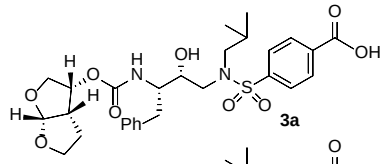 **3a**	12	>1000
2.	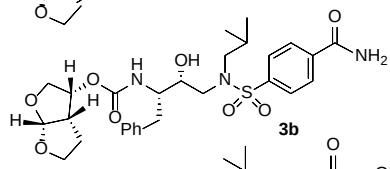 **3b**	8.9	45
3.	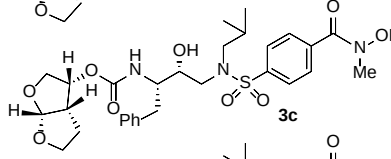 **3c**	192	130
4.	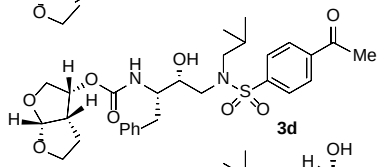 **3d**	9.7	2.0
5.	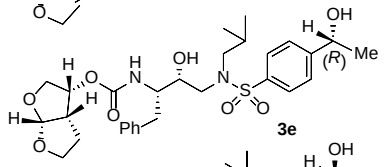 **3e**	9.9	4.0
6.	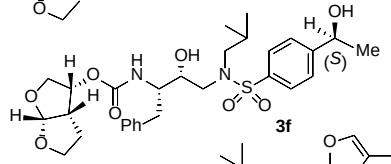 **3f**	46	nt
7.	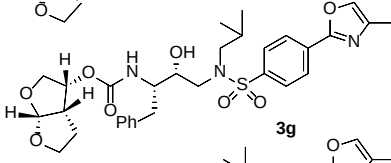 **3g**	27.9	6.2
8.	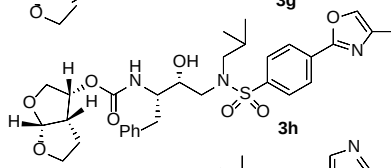 **3h**	49.7	3.9
9.	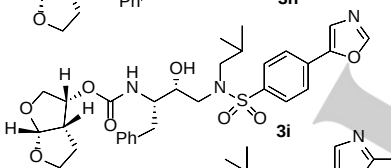 **3i**	126	2.8
10.	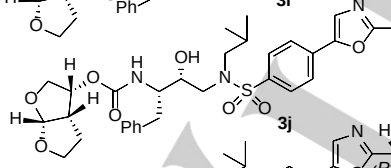 **3j**	119	2.8
11.	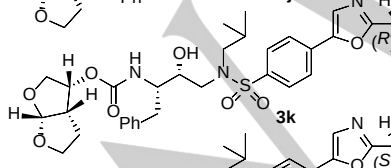 **3k**	37.3	3.2
12.	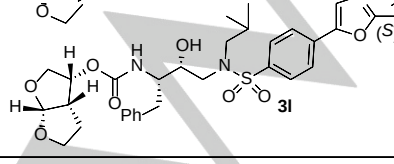 **3l**	21.7	nt

[a]Ki values represents at least 5 data points. Standard error in all cases was less than 7%. Darunavir exhibited K_i = 16 pM. [b]nt = not tested. [c]Values are means of at least three experiments. Standard error in all cases was less than 5%. Darunavir exhibited IC_{50} = 1.6 nM.

Since compound **3g** contains an interesting heterocyclic P2'-ligand, we planned to obtain molecular insight into its binding properties using an X-ray structure. Towards this objective, we determined the X-ray structure of **3g**-bound HIV-1 protease. To further correlate structure with its antiviral properties, we examined both potent oxazole containing PIs (**3g**, **3h**) against DRV-resistant HIV-1 variants. In these assays, MT-4 cells were exposed to wild-type HIV-1 and three drug-resistant variants HIV-$1_{DRV}{}^{R}{}_{20}$, HIV-$1_{DRV}{}^{R}{}_{30}$, and HIV-$1_{DRV}{}^{R}{}_{40}$ and treated with various concentrations of each inhibitor. These DRV-resistant variants HIV-$1_{DRV}{}^{R}{}_{S}$ are highly resistant to all current clinically used PIs including DRV and nucleoside/nucleotide reverse transcriptase inhibitors such as tenofovir. IC_{50} values were determined using p24 assay.[33,34] The results are shown in Table 2. Oxazole derivative **3g** was less potent against HIV_{NL4-3} compared to DRV (3.4 nM *vs* 22 nM). Its fold-change against $HIV_{DRV}{}^{R}{}_{P20}$ is similar to DRV, however, fold-changes against $HIV_{DRV}{}^{R}{}_{P30}$ and $HIV_{DRV}{}^{R}{}_{P40}$ were more than 3-fold and 6-fold lower compared to DRV (fold differences for DRV 71- and >297-fold). Inhibitor **3h** with a hydroxymethyl side chain on the oxazole ring showed similar IC_{50} value as DRV against HIV_{NL4-3}. Its fold-change of antiviral activity against $HIV_{DRV}{}^{R}{}_{20}$ was higher than compound **3g** and DRV, although the fold-changes against $HIV_{DRV}{}^{R}{}_{30}$ and $HIV_{DRV}{}^{R}{}_{40}$ were comparable to DRV. These data indicate an interesting profile for the novel inhibitor **3g** towards DRV-resistant variants to be considered as a starting point for further optimization.

Table 2. Antiviral activity of two novel compounds against highly DRV-resistant HIV-1 variants.

	Mean IC_{50} in nM (fold-change)[a,b,c]		
	DRV	**3g**	**3h**
$HIV\text{-}1_{NL4-3}$	3.4	22	3.0
$HIV\text{-}1_{DRV}{}^{R}{}_{P20}$	43 (13)	320 (15)	260 (88)
$HIV\text{-}1_{DRV}{}^{R}{}_{P30}$	24 (71)	430 (20)	290 (99)
$HIV\text{-}1_{DRV}{}^{R}{}_{P40}$	>1 (> 297)	>1 (> 46)	>1 (> 337)

[a]MT-4 cells (1 x 10^4) were exposed to 50 $TCID_{50}$s of wild-type $HIV\text{-}1_{NL4-3}$, $HIV\text{-}1_{DRV}{}^{R}{}_{P20}$, $HIV\text{-}1_{DRV}{}^{R}{}_{P30}$, or $HIV\text{-}1_{DRV}{}^{R}{}_{P40}$ and cultured in the presence of various concentrations of each PI, and the IC_{50} values were determined using the p24 assay. The amino acid substitutions identified in protease of HIV-$1_{DRV}{}^{R}{}_{P20}$, HIV-$1_{DRV}{}^{R}{}_{P30}$, and HIV-$1_{DRV}{}^{R}{}_{P40}$ compared to $HIV\text{-}1_{NL4-3}$ include L10I/I15V/K20R/L24I/V32I/M36I/M46L/L63P/V82A/L89M; L10I/I15V/K20R/L24I/V32I/M36I/M46L/L63P/K70R/V82A/I84V/L89M and L10I/I15V/K20R/L24I/V32I/L33F/M36I/M46L/I54M/L63P/K70Q/V82I/I84V/L89M, respectively. [b]All assays were conducted in triplicate, and the data shown represent mean values derived from the results of three independent experiments. [c]Standard error in all cases was less than 5%.

X-ray description

To gain molecular insight into interactions of oxazole inhibitors, we co-crystallized inhibitor **3g** (GRL-5311) with wild-type HIV-1 protease and the X-ray structure was refined at 1.30

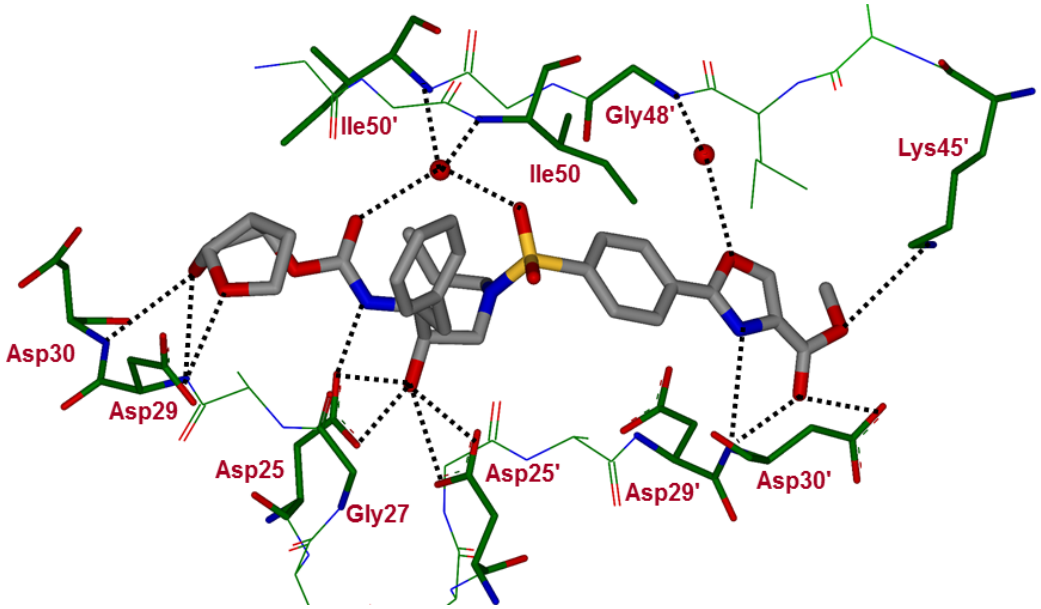

Figure 3. Inhibitor **3g**-bound X-ray structure of HIV-1 protease. The major orientation of the inhibitor is shown. The inhibitor carbon atoms are shown in grey, water molecules are red spheres, and the hydrogen bonds are indicated by dotted lines (PDB ID: 6B4N).

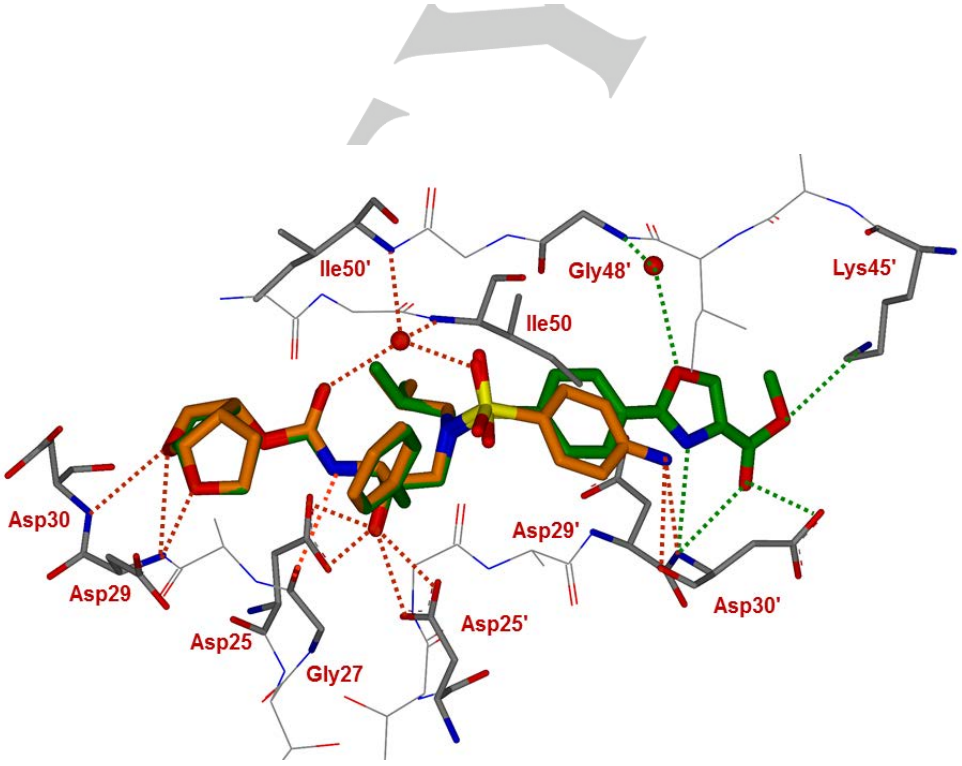

Figure 4. An overlay of X-ray crystal structure of DRV-bound HIV-1 protease (orange) with the X-ray structure of inhibitor **3g** (green)-bound HIV-1 protease.

Å resolution to an R_{work}/R_{free} of 15.4/19.6% (PDB ID: 6B4N). The structure contains HIV-1 protease dimer with inhibitor **3g** bound in a single orientation. The HIV-1 protease dimer structure closely resembles our reported structure of protease-DRV complex with RMSD of 0.22 Å for all Cα atoms.[20] Larger differences between the corresponding Cα atoms were evident in one subunit of the dimer, where the differences of 0.75 Å occurred for residues 53' to 54' in the flap region and 0.77 Å for residues 80' and 81' in the 80s loop. These shifts are probably because the inhibitor **3g** has a larger P2' and P3' substituted oxazole group relative to the P2' ligand of DRV. The inhibitor binds in the active site showing similar interactions for P2-*bis*-THF, the urethane functionality, and the P1-phenylmethyl side chain to those observed for the HIV-1 protease-DRV X-ray structure.[20]

The major differences for inhibitor **3g** interactions with HIV-1 protease are evident in the S2'-subsite where the 4-amino group of DRV replaced by a substituted oxazole group. As shown in Figure 3, the oxazole nitrogen forms a strong hydrogen bond with the backbone NH of Asp30'. Interestingly, the carboxyl group of the ester side chain also forms a strong hydrogen bond with Asp30' backbone NH. The oxygen atom of the oxazole heterocycle forms a water-mediated interaction with Gly48' amide NH. The carbonyl group of the oxazole side chain has two orientations and both stack against the carboxylic acid side chain of Asp30'. In one *S*-trans orientation of the ester, the methoxy oxygen is within hydrogen bonding distance of the Lys45' amine side chain. Furthermore, the aromatic P2'-ring in **3g** has shifted towards the flap region, as shown in the overlay of X-ray structures of DRV-bound HIV-1 protease and inhibitor **3g**-bound HIV-1 protease (Figure 4). The side chain of Asp30' has also shifted toward Asn88 to accommodate the oxazole ring. This heterocyclic core shows good van der Waals interactions with the side chains of Ile47', Asp29', and the main chain of Gly48'. These interactions may be responsible for inhibitor's high affinity for HIV-1 protease.

Conclusions

In conclusion, we have designed, synthesized, and examined a number of HIV-1 PIs containing carboxylic acid derivatives and substituted oxazole derivatives as the P2' ligands. These ligands are designed to enhance interactions with backbone atoms and residue in the S2' subsite. Inhibitor **3b** with 4-carboxamide functionality showed enhanced potency over the carboxylic acid **3a**. The X-ray structure of **3b**-bound HIV-1 protease showed key hydrogen bonding interactions with Asp30' backbone NH. Furthermore, the carboxamide also formed an interesting water-mediated hydrogen bond with the Gly48' carbonyl group. Antiviral activity of **3b** showed that it is highly active against HIV_{AO2} with EC_{50} value of 29 nM. Antiviral activity of **3b** against $HIV\text{-}2_{ROD}$ or $HIV_{DRV}{}^{R}{}_{P20}$ was 30 nM and 97 nM. There was only 2.6-fold increase in its EC_{50} value compared to its EC_{50} against HIV_{WT}. Based upon the X-ray structure of **3b**-bound HIV-1 protease and its biological properties, we have examined a series of derivatives, including stereochemically defined alcohols, ketone, methoxymethylamide, 2-phenyl oxazole derivatives, and 5-phenyl oxazole derivatives. Both methyl ketone **3d** and its reduction products provided very potent enzyme inhibitory and antiviral activity comparable to DRV. Various oxazole derivatives also displayed very potent antiviral activity. In particular, inhibitors **3g** and **3h** with 2-phenyl oxazoles as the P2'-ligand showed very potent antiviral activity. While inhibitor **3h** has shown 10-fold better IC_{50} value compared to inhibitor **3g** against $HIV_{NL4\text{-}3}$, inhibitor **3h** showed similar fold-changes as DRV against $HIV_{DRV}{}^{R}{}_{P30}$ and $HIV_{DRV}{}^{R}{}_{40}$. However, its fold-changes are higher against $HIV_{DRV}{}^{R}{}_{P20}$. While inhibitor **3g** showed IC_{50} value of 22 nM against $HIV_{NL4\text{-}3}$, its fold-changes against DRV-resistant viruses are superior to inhibitor **3h** or DRV. The X-ray crystal structure of **3g**-bound HIV-1 protease revealed new water-mediated hydrogen bonding interactions in the S2'-subsite of HIV-1 protease. Further design and synthesis of new inhibitors using this molecular insight is in progress.

Experimental Section

General

All moisture sensitive reactions were carried out in an oven dried flask under argon atmosphere. All chemicals and reagents were purchased from commercial suppliers and used without further purification. Anhydrous solvents were obtained as follows: anhydrous tetrahydrofuran, diethyl ether, and benzene were distilled from sodium metal under argon. Anhydrous dichloromethane, toluene, methanol, and acetonitrile were dried via distillation from CaH_2 under argon. All other solvents were HPLC grade. ^{1}H NMR and ^{13}C NMR spectra were recorded on Varian INOVA300-1, Bruker Avance ARX-400 and Bruker DRX-500 spectrometers. NMR data are reported as: δ value (chemical shift, *J*-value (Hz), integration, where s = singlet, d = doublet, t = triplet, q = quartet, br = broad). Low resolution mass analyses were performed on a Agilent 1290 Infinity II spectrometer. High Resolution mass analyses were performed at the Purdue University Campus-wide Mass Spectrometry Center. TLC analysis was carried out with SiliCycle 60A-F_{254} plates. Flash chromatography was performed using SiliCycle 230-400 mesh, 60 Å pore diameter silica gel. HPLC analysis was performed on a Agilent 1260 Infinity instrument. All test inhibitors showed purity >95% by HPLC analysis.

4-(*N*-((2*R*,3*S*)-3-((*tert*-Butoxycarbonyl)amino)-2-hydroxy-4-phenylbutyl)-*N*-isobutylsulfamoyl)benzoic acid (7): To a solution of compound **5** (81 mg, 0.156 mmol) in MeOH (14 mL) was added K_2CO_3 (113 mg, 0.392 mmol) and the reaction was stirred at 23 °C for 1 h. The reaction mixture was concentrated under reduced pressure and the residue partitioned between water and EtOAc. The organic layers were dried over anhydrous sodium sulfate, filtered and concentrated. The crude was purified by silica gel flash chromatography (30% EtOAc in *n*-hexane) providing *tert-Butyl ((2S,3R)-4-((4-formyl-N-isobutylphenyl)sulfonamido)-3-hydroxy-1-phenylbutan-2-yl)carbamate* (98% yield). ^{1}H NMR (400 MHz, $CDCl_3$) δ 10.08 (s, 1H), 8.00 (d, *J* = 8.4 Hz, 2H), 7.93 (d, *J* = 8.3 Hz, 2H), 7.41 – 7.11 (m, 5H), 4.67 (d, *J* = 8.2 Hz, 1H), 3.95 – 3.64 (m, 3H), 3.16 (d, *J* = 5.8 Hz, 2H), 3.03 – 2.71 (m, 4H), 1.96 – 1.73 (m, 1H), 1.34 (s, 9H), 0.86 (dd, *J* = 8.8, 6.7 Hz, 6H). ^{13}C NMR (100 MHz, $CDCl_3$) δ 190.9, 156.4, 144.2, 138.9, 137.8, 130.3, 129.6, 128.7, 128.1, 127.8, 126.7, 80.1, 72.7, 58.1, 55.1, 53.2, 35.7, 28.4, 27.2, 20.2, 20.0. LRMS-ESI (*m/z*): 527.2 $[M+Na]^+$. This aldehyde intermediate (41 mg, 0.081 mmol) was dissolved in *t*-BuOH (5 mL) and 2-methyl-2-butene (2 mL) was added at 23 °C. 2.6 mL of a stock solution obtained by dissolving $NaH_2PO_4{\cdot}H_2O$ (600 mg)

and $NaClO_2$ (600 mg) in 6 mL of water were added and the reaction mixture was stirred at 23 °C for 50 min. Water (3 mL) was added and the reaction mixture was extracted with EtOAc. The organic layers were washed with brine, dried over anhydrous sodium sulfate, filtered and concentrated. The crude was purified by silica gel flash chromatography (5% to 10% MeOH in CH_2Cl_2) providing compound **7** as a white solid (95% yield). ^{1}H NMR (400 MHz, CD_3OD) δ 8.17 (d, *J* = 8.3 Hz, 2H), 7.92 (d, *J* = 8.3 Hz, 2H), 7.30 – 7.18 (m, 3H), 7.18 – 7.09 (m, 2H), 3.71 (t, *J* = 7.1 Hz, 1H), 3.64 – 3.53 (m, 1H), 3.42 (dd, *J* = 15.0, 1.9 Hz, 1H), 3.20 – 3.01 (m, 2H), 2.94 (dd, *J* = 13.7, 6.7 Hz, 1H), 2.54 (dd, *J* = 13.7, 10.8 Hz, 1H), 2.10 – 1.95 (m, 1H), 1.36 – 1.21 (m, 9H), 0.89 (dd, *J* = 15.4, 6.6 Hz, 6H). ^{13}C NMR (100 MHz, DMSO) δ 168.3, 158.1, 144.9, 140.3, 135.8, 131.5, 130.6, 129.3, 128.7, 127.2, 80.2, 74.0, 58.3, 57.0, 53.6, 37.4, 28.8, 27.9, 20.5. LRMS-ESI (*m/z*): 521.2 $[M+H]^+$, 543.1 $[M+Na]^+$.

***tert*-Butyl ((2*S*,3*R*)-3-hydroxy-4-((*N*-isobutyl-4-(methoxy(methyl)carbamoyl)phenyl)sulfonamido)-1-phenylbutan-2-yl)carbamate (8):** Compound **7** (58 mg, 0.111 mmol) was dissolved in dry CH_2Cl_2 (6 mL) and *N*-methyl morpholine (27 μL, 0.244 mmol) was added. The solution was cooled to -15 °C and *i*BuOCOCl (16 μL, 0.122 mmol) was added. The reaction mixture was stirred at -15 °C for 15 min, then *N,O*-dimethylhydroxylamine hydrochloride (11 mg, 0.113 mmol) was added and the reaction was stirred at 23 °C for 12 h. The mixture was then partitioned between water and CH_2Cl_2. Organic layer was dried over anhydrous sodium sulfate, filtered and concentrated. The crude was purified by silica gel flash chromatography (5% MeOH in CH_2Cl_2) providing compound **8** as a white solid (76% yield). ^{1}H NMR (400 MHz, $CDCl_3$) δ 7.99 – 7.70 (m, 4H), 7.39 – 7.10 (m, 5H), 4.69 (d, *J* = 7.6 Hz, 1H), 3.96 – 3.68 (m, 3H), 3.51 (s, 3H), 3.37 (s, 3H), 3.13 (d, *J* = 5.7 Hz, 2H), 3.05 – 2.80 (m, 4H), 1.94 – 1.75 (m, 1H), 1.46 – 1.20 (m, 9H), 0.86 (dd, *J* = 11.1, 6.6 Hz, 6H). ^{13}C NMR (100 MHz, $CDCl_3$) δ 168.3, 156.3, 140.5, 138.4, 138.0, 129.7, 129.0, 128.6, 127.2, 126.6, 79.9, 72.8, 61.5, 58.4, 55.1, 53.6, 35.6, 33.4, 28.4, 27.2, 20.2, 20.0. LRMS-ESI (*m/z*): 564.3 $[M+H]^+$, 586.2 $[M+Na]^+$.

Methyl 2-(4-(*N*-((2*R*,3*S*)-3-((*tert*-butoxycarbonyl)amino)-2-hydroxy-4-phenylbutyl)-*N*-isobutylsulfamoyl)phenyl)oxazole-4-carboxylate (9): Compound **7** (32 mg, 0.0615 mmol) was dissolved in dry DMF (4 mL) and the solution was cooled to 0 °C. EDCI (14 mg, 0.074 mmol), HOBt (10 mg, 0.074 mmol), *N,N*-DIPEA (20 mL, 0.153 mmol) and DL-serine methyl ester hydrochloride (12 mg, 0.074 mmol) were sequentially added to the solution and the reaction mixture was stirred at 23 °C for 16 h. Water was added and the reaction mixture was extracted with EtOAc. Organic layers were dried over anhydrous sodium sulfate, filtered and concentrated. The crude was purified by silica gel flash chromatography (EtOAc) providing methyl *(4-(N-((2R,3S)-3-((tert-butoxycarbonyl)amino)-2-hydroxy-4-phenylbutyl)-N-isobutylsulfamoyl)benzoyl)serinate* as a colourless oil (91% yield). ^{1}H NMR (400 MHz, $CDCl_3$) δ 7.94 (d, *J* = 8.4 Hz, 2H), 7.83 (d, *J* = 8.3 Hz, 2H), 7.42 – 7.13 (m, 5H), 4.88 (dt, *J* = 7.0, 3.3 Hz, 1H), 4.67 (d, *J* = 8.1 Hz, 1H), 4.08 – 4.00 (m, 2H), 3.92 – 3.86 (m, 1H), 3.86 – 3.68 (m, 5H), 3.13 (d, *J* = 5.7 Hz, 2H), 3.04 – 2.82 (m, 4H), 2.63 (br, 1H), 1.92 – 1.78 (m, 1H), 1.67 (s, 1H), 1.65 – 1.51 (m, 1H), 1.34 (s, 9H), 0.87 (dd, *J* = 10.6, 6.6 Hz, 6H).

The above intermediate (70 mg, 0.113 mmol) was dissolved in dry CH_2Cl_2 (5 mL) and the solution was cooled to -78 °C. DAST (17 μL, 0.124 mmol) was added dropwise. The reaction mixture was stirred at -78 °C for 30 min (TLC monitoring in 100% EtOAc) and then quenched with K_2CO_3 and passed quickly through a silica gel column pre-treated with triethylamine and eluted with EtOAc. The crude material recovered from the column was dried under reduced pressure and dissolved in dry CH_2Cl_2 (5 mL) and the resulting solution was cooled to 0 °C. $BrCCl_3$ (13 μL, 0.124 mmol) and DBU (19 μL, 0.124 mmol) were sequentially added and the reaction mixture was then stirred at 23 °C for 2.5 h. Solvents were evaporated under reduced pressure and the residue was purified by silica gel flash chromatography (50% EtOAc in *n*-hexane) providing compound **9** as a white solid (64% yield over 2 steps). ^{1}H NMR (400 MHz, $CDCl_3$) δ 8.35 (s, 1H), 8.24 (d, *J* = 8.5 Hz, 2H), 7.87 (d, *J* = 8.5 Hz, 2H), 7.40 – 7.16 (m, 5H), 4.67 (d, *J* = 7.7 Hz, 1H), 3.97 (s, 3H), 3.94 – 3.86 (m, 1H), 3.86 – 3.70 (m, 2H), 3.16 (d, *J* = 5.8 Hz, 2H), 3.08 – 2.83 (m, 4H), 1.94 – 1.80 (m, 1H), 1.34 (s, 9H), 0.86 (dd, *J* = 11.0, 6.6 Hz, 6H). ^{13}C NMR (100 MHz, $CDCl_3$) δ 161.5, 160.9, 156.3, 144.7, 141.2, 137.9, 135.1, 130.2, 129.7, 128.7, 128.0, 127.6, 126.7, 108.9, 80.0, 72.8, 58.3, 55.1, 53.3, 52.6, 35.6, 28.4, 27.2, 20.2, 20.0. LRMS-ESI (*m/z*): 624.2 $[M+Na]^+$, 502.1 $[M-Boc+H]^+$.

***tert*-Butyl ((2*S*,3*R*)-3-hydroxy-4-((*N*-isobutyl-4-(oxazol-5-yl)phenyl)sulfonamido)-1-phenylbutan-2-yl)carbamate (10):** Compound **5** (52 mg, 0.086 mmol) and TosMIC (40 mg, 0.206 mmol) were dissolved in MeOH (3 mL) in a sealed tube and K_2CO_3 (76 mg, 0.548 mmol) was added. The reaction mixture was stirred at 55 °C for 1.5 h (TLC monitoring). The reaction mixture was then cooled to room temperature and filtered on a celite pad. The crude residue was purified by silica gel flash chromatography (20% to 50% EtOAc in *n*-hexane) providing compound **10** as a white solid (96% yield). ^{1}H NMR (500 MHz, $CDCl_3$) δ 8.04 (s, 1H), 7.88 (d, *J* = 8.5 Hz, 2H), 7.82 (d, *J* = 8.4 Hz, 2H), 7.55 (s, 1H), 7.45 – 7.18 (m, 5H), 4.81 (d, *J* = 8.4 Hz, 1H), 3.96 – 3.75 (m, 2H), 3.32 – 3.16 (m, 2H), 3.12 – 2.80 (m, 4H), 1.98 – 1.81 (m, 1H), 1.35 (s, 9H), 0.93 (dd, *J* = 11.2, 6.6 Hz, 6H). ^{13}C NMR (125 MHz, $CDCl_3$) δ 156.3, 151.6, 150.0, 138.4, 137.9, 131.7, 129.6, 128.6, 128.2, 126.6, 124.9, 124.0, 79.9, 72.8, 58.4, 54.9, 53.5, 35.6, 28.4, 27.2, 20.2, 20.0.

***tert*-Butyl ((2*S*,3*R*)-4-((4-(2-acetyloxazol-5-yl)-*N*-isobutylphenyl)sulfonamido)-3-hydroxy-1-phenylbutan-2-yl)carbamate (11):** Compound **10** (42 mg, 0.0775 mmol) was dissolved in dry THF (2 mL) and the resulting solution was cooled to – 15 °C. Then *i*PrMgCl (2.0 M solution in THF, 116 μL, 0.232 mmol) was added dropwise and the mixture was stirred for 40 min at -15 °C. *N*-Methoxy-*N*-methylacetamide (25 μL, 0.232 mmol) was added and the reaction mixture was allowed to slowly reach 23 °C and stirred for 5 h. The reaction was quenched with a saturated solution of NH_4Cl and extracted with EtOAc. The organic layers were dried over anhydrous sodium sulfate, filtered and concentrated. The crude was purified by silica gel flash chromatography (20% to 50% EtOAc in *n*-hexane) providing compound **11** as an amorphous white solid (79% yield). ^{1}H NMR (400 MHz, $CDCl_3$) δ 7.65 (s, 1H), 7.40 – 7.14 (m, 5H), 4.62 (br, 1H), 3.97 – 3.66 (m, 3H), 3.16 (d, *J* = 5.6 Hz, 2H), 3.06 – 2.83 (m, 4H), 2.72 (s, 3H), 1.96 – 1.79 (m, 1H), 1.35 (s, 9H), 0.88 (dd, *J* = 11.1, 6.7 Hz, 6H), 8.01 – 7.79 (m, 4H).

4-(*N*-((2*R*,3*S*)-3-(((((3*R*,3a*S*,6a*R*)-Hexahydrofuro[2,3-*b*]furan-3-yl)oxy)carbonyl)amino)-2-hydroxy-4-phenylbutyl)-*N*-isobutylsulfamoyl)benzoic acid (3a): Compound **7** (11.5 mg, 0.0221 mmol) was dissolved in dry CH_2Cl_2 (3 mL) and TFA (400 μL) was added. The resulting mixture was stirred at 23 °C for 3 h. Solvents were evaporated under reduced pressure, then CH_2Cl_2 (5 mL) was added and evaporated twice to provide the corresponding Boc-deprotected compound, which was carried on without further purification. The compound was dissolved in a mixure of MeCN (4 mL) and water (0.4 mL), then *N,N*-DIPEA (39 μL, 0.221 mmol) and activated *bis*-THF carbonate **6** (7.8 mg, 0.0252 mmol) were sequentially added and the reaction mixture was stirred at 23 °C for 3 days. Volatiles were evaporated under reduced pressure and the crude residue was purified by HPLC to provide pure **3a** as a white solid (89% yield over 2 steps). ^{1}H NMR (500 MHz, CD_3OD) δ 8.22 (d, *J* = 8.4 Hz, 2H), 7.97 (d, *J* = 8.4 Hz, 2H), 7.35 – 7.24 (m, 4H), 7.24 – 7.13 (m, 1H), 5.62 (d, *J* = 5.2 Hz, 1H), 3.97 (dd, *J* = 9.7, 6.0 Hz, 1H), 3.85 – 3.74 (m, 4H), 3.74 – 3.63 (m, 1H), 3.55 – 3.47 (m, 1H), 3.27 – 3.17 (m, 2H), 3.08 (dd, *J* = 15.0, 8.3 Hz, 1H), 2.98 (dd, *J* = 13.7, 6.7 Hz, 1H), 2.94 – 2.86 (m, 1H), 2.55 (dd, *J* = 13.8, 10.9 Hz, 1H), 2.14 – 2.00 (m, 1H), 1.59 – 1.46 (m, 1H), 1.41 – 1.28 (m, 1H), 0.94 (dd, *J* = 26.3, 6.6 Hz, 6H). ^{13}C NMR (125 MHz, CD_3OD) δ 167.2, 156.7, 143.7, 139.2, 130.5, 129.5, 128.3, 127.6, 126.3, 109.8, 73.6, 73.2, 71.1, 69.7, 57.4, 56.5, 52.5, 45.9, 36.1, 26.9, 26.0, 19.4.

(3*R*,3a*S*,6a*R*)-Hexahydrofuro[2,3-*b*]furan-3-yl ((2*S*,3*R*)-4-((4-carbamoyl-*N*-isobutylphenyl)sulfonamido)-3-hydroxy-1-phenylbutan-2-yl)carbamate (3b): Compound **3a** (3.4 mg, 0.0059 mmol) was dissolved in THF (4 mL) and pyridine (0.5 mL), Boc_2O (2 mg, 0.0092 mmol) and $(NH_4)_2CO_3$ (1 mg, 0.0104 mmol) were sequentially added. The reaction mixture was stirred at 23 °C for 14 h and then concentrated under reduced pressure. The residue was purified by silica gel flash chromatography (10% MeOH in CH_2Cl_2) providing **3b** as a white solid (76% yield). ^{1}H NMR (400 MHz, $CDCl_3$) δ 7.95 (d, *J* = 8.4 Hz, 2H), 7.84 (d, *J* = 8.3 Hz, 2H), 7.36 – 7.12 (m, 5H), 6.34 (br, 1H), 5.82 (br, 1H), 5.64 (d, *J* = 5.2 Hz, 1H), 5.03 – 4.87 (m, 2H), 3.98 – 3.79 (m, 4H), 3.76 – 3.58 (m, 2H), 3.51 – 3.41 (m, 1H), 3.21 – 3.02 (m, 2H), 3.00 – 2.84 (m, 3H), 2.78 (dd, *J* = 13.9, 9.0 Hz, 1H), 1.85 (dt, *J* = 13.6, 6.6 Hz, 1H), 1.74 – 1.56 (m, 2H), 1.55 – 1.42 (m, 1H), 0.90 (dd, *J* = 9.5, 6.6 Hz, 6H). LRMS-ESI (*m/z*): 576.3 $[M+H]^+$, 598.2 $[M+Na]^+$; HRMS-ESI (*m/z*) $[M+Na]^+$ calculated for $C_{28}H_{37}N_3O_8SNa$ 598.2199, found 598.2206.

(3*R*,3a*S*,6a*R*)-Hexahydrofuro[2,3-*b*]furan-3-yl ((2*S*,3*R*)-3-hydroxy-4-((*N*-isobutyl-4-(methoxy(methyl)carbamoyl)phenyl)sulfonamido)-1-phenylbutan-2-yl)carbamate (3c): Compound **8** (6.5 mg, 0.0115 mmol) was dissolved in dry CH_2Cl_2 (3 mL) and TFA (200 μL) was added to the solution. The reaction mixture was stirred at 23 °C for 2 h. Solvents were evaporated under reduced pressure, then CH_2Cl_2 (5 mL) was added and evaporated twice to provide the corresponding Boc-deprotected compound, which was carried on without further purification. The compound was dissolved in MeCN (4 mL), then *N,N*-DIPEA (20 μL, 0.115 mmol) and activated *bis*-THF carbonate **6** (3.4 mg, 0.0115 mmol) were sequentially added and the reaction mixture was stirred at 23 °C for 5 days. Volatiles were evaporated under reduced pressure and the residue was purified by silica gel flash chromatography (50% EtOAc in *n*-hexane) to provide **3c** as a white solid (73% yield over 2 steps). ^{1}H NMR (400 MHz, $CDCl_3$) δ 7.87 – 7.75 (m, 4H), 7.39 – 7.11 (m, 5H), 5.64 (d, *J* = 5.2 Hz, 1H), 5.03 (dd, *J* = 14.0, 6.2 Hz, 1H), 4.92 (d, *J* = 8.5 Hz, 1H), 4.00 – 3.80 (m, 4H), 3.75 – 3.62 (m, 2H), 3.59 – 3.47 (m, 4H), 3.39 (s, 3H), 3.21 (dd, *J* = 15.0, 8.5 Hz, 1H), 3.14 – 2.96 (m, 3H), 2.95 – 2.71 (m, 3H), 1.93 – 1.78 (m, 1H), 1.50 – 1.38 (m, 2H), 0.90 (dd, *J* = 20.8, 6.6 Hz, 6H).

(3*R*,3a*S*,6a*R*)-Hexahydrofuro[2,3-*b*]furan-3-yl ((2*S*,3*R*)-4-((4-acetyl-*N*-isobutylphenyl)sulfonamido)-3-hydroxy-1-phenylbutan-2-yl)carbamate (3d): Compound **8** (35 mg, 0.062 mmol) was dissolved in dry THF (2.5 mL) and the resulting solution was cooled to -78 °C. MeMgBr (3M solution in Et_2O, 105 μL, 0.310 mmol) was added dropwise and the reaction mixture was stirred at -78 °C for 4 h and then quenched with a saturated solution of NH_4Cl. The mixture was extracted with EtOAc and the organic layers were dried over anhydrous sodium sulfate, filtered and concentrated. The crude was purified by silica gel flash chromatography (50% EtOAc in *n*-hexane) providing *tert-butyl ((2S,3R)-4-((4-acetyl-N-isobutylphenyl)sulfonamido)-3-hydroxy-1-phenylbutan-2-yl)carbamate* (98% yield). ^{1}H NMR (400 MHz, $CDCl_3$) δ 8.07 (d, *J* = 8.3 Hz, 2H), 7.88 (d, *J* = 8.3 Hz, 2H), 7.37 – 7.14 (m, 5H), 4.70 (d, *J* = 7.5 Hz, 1H), 3.92 (br, 1H), 3.86 – 3.69 (m, 2H), 3.23 – 3.12 (m, 2H), 3.07 – 2.82 (m, 4H), 2.66 (s, 3H), 1.97 – 1.72 (m, 2H), 1.36 (s, 9H), 0.89 (dd, *J* = 9.9, 6.6 Hz, 6H). ^{13}C NMR (100 MHz, $CDCl_3$) δ 196.89, 156.37, 142.78, 140.14, 137.86, 129.65, 129.10, 128.69, 127.77, 126.68, 80.05, 72.71, 58.30, 55.08, 53.35, 35.68, 28.39, 27.21, 27.01, 20.20, 20.01.
The above methyl ketone intermediate was then Boc-deprotected and submitted to coupling with the activated *bis*-THF derivative **6** as described for compound **3c**, providing pure compound **3d** as an amorphous white solid (78% yield over 2 steps). ^{1}H NMR (400 MHz, $CDCl_3$) δ 8.08 (d, *J* = 8.4 Hz, 2H), 7.87 (d, *J* = 8.4 Hz, 2H), 7.35 – 7.15 (m, 5H), 5.65 (d, *J* = 5.2 Hz, 1H), 5.02 (dd, *J* = 14.0, 6.2 Hz, 1H), 4.92 (d, *J* = 8.3 Hz, 1H), 4.01 – 3.81 (m, 4H), 3.76 – 3.62 (m, 2H), 3.55 (br, 1H), 3.26 – 3.14 (m, 1H), 3.13 – 2.96 (m, 3H), 2.96 – 2.74 (m, 3H), 2.66 (s, 3H), 1.92 – 1.75 (m, 1H), 1.74 – 1.40 (m, 2H), 0.90 (dd, *J* = 19.9, 6.6 Hz, 6H). LRMS-ESI (*m/z*): 597.1 $[M+Na]^+$; HRMS-ESI (*m/z*) $[M+Na]^+$ calculated for $C_{29}H_{38}N_2O_8SNa$ 597.2247, found 597.2243.

(3*R*,3a*S*,6a*R*)-Hexahydrofuro[2,3-*b*]furan-3-yl ((2*S*,3*R*)-3-hydroxy-4-((4-((*R*)-1-hydroxyethyl)-*N*-isobutylphenyl)sulfonamido)-1-phenylbutan-2-yl)carbamate (3e): Compound **3d** (3 mg, 0.0052 mmol) was dissolved in dry CH_2Cl_2 (0.5 mL) and Et_3N (280 μL) and HCO_2H (140 μL) were added at 0 °C. After stirring for 30 min, Noyori asymmetric transfer hydrogenation catalyst RuCl[(*R,R*)-TsDPEN](mesitylene) (0.5 mol%) was added and the reaction mixture was stirred at 23 °C for 7 h. The reaction mixture was then quenched saturated $NaHCO_3$ and extracted with CH_2Cl_2. The organic layers were dried over anhydrous sodium sulfate, filtered and concentrated. The crude was purified by silica gel flash chromatography (20% to 60% EtOAc in *n*-hexane) providing **3e** as a white solid (94% yield). ^{1}H NMR (500 MHz, $CDCl_3$) δ 7.81 (d, *J* = 8.3 Hz, 2H), 7.60 (d, *J* = 8.2 Hz, 2H), 7.41 – 7.21 (m, 5H), 5.70 (d, *J* = 5.2 Hz, 1H), 5.11 – 4.93 (m, 3H), 4.04 – 3.97 (m, 1H), 3.96 – 3.84 (m, 3H), 3.80 – 3.66 (m, 2H), 3.27 – 3.11 (m, 2H), 3.11 – 3.00 (m, 2H), 3.00 – 2.79 (m, 3H), 1.96 – 1.82 (m, 1H), 1.77 – 1.65 (m, 1H), 1.58 (d, *J* = 6.5 Hz, 3H), 1.55 – 1.46 (m, 1H), 0.98 (dd, *J* = 23.7, 6.6 Hz, 6H). ^{13}C NMR (125 MHz, $CDCl_3$) δ 155.9, 151.7, 138.0, 137.2, 129.8, 129.0, 128.1, 127.1, 126.6, 109.7, 73.9, 73.3, 71.3, 70.0, 60.9, 59.4, 55.5, 54.3, 45.8, 36.1, 27.8, 26.3, 25.9, 20.6,

20.3. LRMS-ESI (*m/z*): 577.2 $[M+H]^+$, 599.3 $[M+Na]^+$; HRMS-ESI (*m/z*) $[M+Na]^+$ calculated for $C_{29}H_{40}N_2O_8SNa$ 599.2404, found 599.2408. HPLC analysis: Chiralpak IA-3 column, 10% isopropanol in *n*-hexane, flow = 1 mL/min, t = 24 °C, λ = 254 nm, rt = 32.1 min, *dr* 98:2.

(3*R*,3a*S*,6a*R*)-Hexahydrofuro[2,3-*b*]furan-3-yl ((2*S*,3*R*)-3-hydroxy-4-((4-((*S*)-1-hydroxyethyl)-*N*-isobutylphenyl)sulfonamido)-1-phenylbutan-2-yl)carbamate (3f): Compound **3f** was obtained from **3d** following the same procedure described for compound **3e** employing RuCl(*p*-cymene)[(*S,S*)-Ts-DPEN] as the catalyst. Compound **3f** was obtained in 98% yield. ^{1}H NMR (500 MHz, $CDCl_3$) δ 7.81 (d, *J* = 8.2 Hz, 2H), 7.60 (d, *J* = 8.1 Hz, 2H), 7.41 – 7.18 (m, 5H), 5.70 (d, *J* = 5.2 Hz, 1H), 5.10 – 4.90 (m, 3H), 4.04 – 3.97 (m, 1H), 3.97 – 3.87 (m, 3H), 3.79 – 3.64 (m, 3H), 3.23 (dd, *J* = 15.1, 8.5 Hz, 1H), 3.14 (dd, *J* = 14.2, 3.8 Hz, 1H), 3.11 – 3.02 (m, 2H), 3.00 – 2.93 (m, 1H), 2.92 – 2.80 (m, 2H), 2.20 (br, 1H), 1.96 – 1.85 (m, 1H), 1.76 – 1.64 (m, 1H), 1.58 (d, *J* = 6.5 Hz, 3H), 1.55 – 1.46 (m, 1H), 0.98 (dd, *J* = 24.1, 6.6 Hz, 6H). ^{13}C NMR (125 MHz, $CDCl_3$) δ 155.9, 151.6, 138.0, 137.3, 129.8, 129.0, 128.0, 127.1, 126.6, 109.7, 73.9, 73.3, 71.3, 70.0, 59.4, 55.6, 54.3, 45.8, 36.1, 28.3, 27.8, 26.3, 25.9, 20.6, 20.3. LRMS-ESI (*m/z*): 577.2 $[M+H]^+$, 599.2 $[M+Na]^+$; HRMS-ESI (*m/z*) $[M+Na]^+$ calculated for $C_{29}H_{40}N_2O_8SNa$ 599.2404, found 599.2408. HPLC analysis: Chiralpak IA-3 column, 10% isopropanol in *n*-hexane, flow = 1 mL/min, t = 24 °C, λ = 254 nm, rt = 34.6 min, *dr* 98:2.

Methyl 2-(4-(*N*-((2*R*,3*S*)-3-(((((3*R*,3a*S*,6a*R*)-hexahydrofuro[2,3-*b*]furan-3-yl)oxy)carbonyl)amino)-2-hydroxy-4-phenylbutyl)-*N*-isobutylsulfamoyl)phenyl)oxazole-4-carboxylate (3g): Compound **3g** was obtained from compound **9** and activated *bis*-THF derivative **6** following the same procedure described for compound **3c** (61% yield over 2 steps). ^{1}H NMR (500 MHz, $CDCl_3$) δ 8.42 (s, 1H), 8.33 (d, *J* = 8.5 Hz, 2H), 7.95 (d, *J* = 8.5 Hz, 2H), 7.43 – 7.17 (m, 5H), 5.71 (d, *J* = 5.2 Hz, 1H), 5.09 (dd, *J* = 14.2, 6.3 Hz, 1H), 5.01 (d, *J* = 8.4 Hz, 1H), 4.13 – 3.98 (m, 4H), 3.98 – 3.84 (m, 3H), 3.85 – 3.69 (m, 2H), 3.64 (s, 1H), 3.29 (dd, *J* = 15.1, 8.3 Hz, 1H), 3.22 – 3.05 (m, 3H), 3.03 – 2.93 (m, 2H), 2.87 (dd, *J* = 14.0, 9.1 Hz, 1H), 1.96 – 1.81 (m, 1H), 1.78 – 1.61 (m, 1H), 1.59 – 1.45 (m, 1H), 0.96 (dd, *J* = 25.2, 6.6 Hz, 6H). ^{13}C NMR (125 MHz, $CDCl_3$) δ 161.6, 160.9, 155.7, 144.8, 140.8, 137.7, 135.1, 130.4, 129.5, 128.8, 128.1, 127.7, 126.9, 109.5, 73.7, 72.9, 71.0, 69.8, 58.7, 55.4, 53.7, 52.7, 45.6, 35.8, 27.4, 26.0, 20.3, 20.0. LRMS-ESI (*m/z*): 658.2 $[M+H]^+$, 680.3 $[M+Na]^+$.

(3*R*,3a*S*,6a*R*)-Hexahydrofuro[2,3-*b*]furan-3-yl ((2*S*,3*R*)-3-hydroxy-4-((4-(4-(hydroxymethyl)oxazol-2-yl)-*N*-isobutylphenyl)sulfonamido)-1-phenylbutan-2-yl)carbamate (3h): Compound **9** (8.5 mg, 0.014 mmol) was dissolved in absolute EtOH (3 mL) and the resulting solution was cooled to 0 °C. $NaBH_4$ (1.6 mg, 0.042 mmol) was added and the reaction mixture was stirred at 23 °C for 24 h. The reaction was quenched with saturated aqueous NH_4Cl and extracted with EtOAc. The organic layers were dried over anhydrous sodium sulfate, filtered and concentrated. The crude was purified by silica gel flash chromatography (60% EtOAc in *n*-hexane) providing the corresponding alcohol derivative (65% yield). This intermediate underwent Boc-deprotection and coupling with the *bis*-THF derivative **6** as described for compound **3c** (60% yield over 2 steps). ^{1}H NMR (500 MHz, $CDCl_3$) δ 8.17 (d, *J* = 8.5 Hz, 2H), 7.86 (d, *J* = 8.6 Hz, 2H), 7.73 (s, 1H), 7.36 – 7.11 (m, 5H), 5.64 (d, *J* = 5.2 Hz, 1H), 5.01 (dd, *J* = 14.2, 6.3 Hz, 1H), 4.94 (d, *J* = 8.5 Hz, 1H), 4.70 (s, 2H), 3.96 (dd, *J* = 9.6, 6.3 Hz, 1H), 3.94 – 3.77 (m, 3H), 3.78 – 3.61 (m, 3H), 3.56 (s, 1H), 3.20 (dd, *J* = 15.2, 8.4 Hz, 1H), 3.14 – 2.98 (m, 3H), 2.96 – 2.84 (m, 2H), 2.84 – 2.74 (m, 1H), 1.91 – 1.79 (m, 1H), 1.71 – 1.53 (m, 1H), 1.52 – 1.41 (m, 1H), 0.98 – 0.84 (m, 6H). ^{13}C NMR (125 MHz, $CDCl_3$) δ 160.5, 155.7, 142.4, 139.9, 137.7, 136.4, 131.4, 129.5, 128.8, 128.1, 127.2, 126.9, 109.5, 73.7, 72.9, 70.9, 69.8, 58.8, 57.3, 55.4, 53.7, 45.5, 35.8, 27.4, 26.0, 20.3, 20.1. LRMS-ESI (*m/z*): 630.3 $[M+H]^+$, 652.2 $[M+Na]^+$.

(3*R*,3a*S*,6a*R*)-Hexahydrofuro[2,3-*b*]furan-3-yl ((2*S*,3*R*)-3-hydroxy-4-((*N*-isobutyl-4-(oxazol-5-yl)phenyl)sulfonamido)-1-phenylbutan-2-yl)carbamate (3i): Compound **3i** was obtained from compound **10** and activated *bis*-THF derivative **6** following the same procedure described for compound **3c** (47% over 2 steps). ^{1}H NMR (500 MHz, $CDCl_3$) δ 8.00 (s, 1H), 7.84 (d, *J* = 8.7 Hz, 2H), 7.80 (d, *J* = 8.6 Hz, 2H), 7.52 (s, 1H), 7.33 – 7.26 (m, 2H), 7.25 – 7.17 (m, 3H), 5.64 (d, *J* = 5.2 Hz, 1H), 5.09 – 4.95 (m, 2H), 4.01 – 3.79 (m, 4H), 3.79 – 3.54 (m, 3H), 3.20 (dd, *J* = 15.1, 8.4 Hz, 1H), 3.14 – 2.96 (m, 3H), 2.96 – 2.87 (m, 2H), 2.86 – 2.70 (m, 1H), 1.93 – 1.78 (m, 1H), 1.74 – 1.56 (m, 1H), 1.50 – 1.39 (m, 1H), 0.90 (dd, *J* = 22.2, 6.6 Hz, 6H). ^{13}C NMR (125 MHz, $CDCl_3$) δ 155.4, 151.4, 149.6, 137.7, 137.4, 131.7, 129.2, 128.5, 128.0, 126.5, 124.7, 123.9, 109.2, 73.4, 72.7, 70.7, 69.5, 58.5, 55.1, 53.5, 45.3, 35.5, 27.1, 25.7, 20.0, 19.7. LRMS-ESI (*m/z*): 600.3 $[M+H]^+$, 622.2 $[M+Na]^+$; HRMS-ESI (*m/z*) $[M+Na]^+$ calculated for $C_{30}H_{37}N_3O_8SNa$ 622.2199, found 622.2205.

(3*R*,3a*S*,6a*R*)-Hexahydrofuro[2,3-*b*]furan-3-yl ((2*S*,3*R*)-4-((4-(2-acetyloxazol-5-yl)-*N*-isobutylphenyl)sulfonamido)-3-hydroxy-1-phenylbutan-2-yl)carbamate (3j): Compound **3j** was obtained from compound **11** and activated *bis*-THF derivative **6** following the same procedure described for compound **3c** (80% over 2 steps). ^{1}H NMR (500 MHz, $CDCl_3$) δ 7.92 (d, *J* = 8.4 Hz, 2H), 7.86 (d, *J* = 8.5 Hz, 2H), 7.66 (s, 1H), 7.35 – 7.26 (m, 3H), 7.26 – 7.17 (m, 2H), 5.64 (d, *J* = 5.2 Hz, 1H), 5.01 (dd, *J* = 14.0, 6.1 Hz, 1H), 5.00 – 4.92 (m, 1H), 4.00 – 3.80 (m, 4H), 3.75 – 3.62 (m, 2H), 3.59 (s, 1H), 3.21 (dd, *J* = 15.2, 8.4 Hz, 1H), 3.15 – 2.97 (m, 3H), 2.95 – 2.85 (m, 2H), 2.80 (dd, *J* = 13.8, 9.2 Hz, 1H), 2.72 (s, 3H), 1.85 (dt, *J* = 13.3, 6.8 Hz, 1H), 1.73 – 1.56 (m, 1H), 1.51 – 1.39 (m, 1H), 0.90 (dd, *J* = 22.9, 6.6 Hz, 6H). ^{13}C NMR (125 MHz, $CDCl_3$) δ 185.6, 158.0, 155.8, 152.4, 139.5, 137.6, 130.9, 129.5, 128.8, 128.4, 126.9, 126.1, 126.0, 109.5, 73.8, 72.9, 71.0, 69.8, 58.7, 55.4, 53.7, 45.6, 35.8, 27.4, 26.9, 26.0, 20.3, 20.0. LRMS-ESI (*m/z*): 664.2 $[M+Na]^+$; HRMS-ESI (*m/z*) $[M+Na]^+$ calculated for $C_{32}H_{39}N_3O_9SNa$ 664.2305, found 664.2314.

(3*R*,3a*S*,6a*R*)-Hexahydrofuro[2,3-*b*]furan-3-yl ((2*S*,3*R*)-3-hydroxy-4-((4-(2-((*R*)-1-hydroxyethyl)oxazol-5-yl)-*N*-isobutylphenyl)sulfonamido)-1-phenylbutan-2-yl)carbamate (3k): Compound **3k** was obtained from compound **3j** following the same procedure described for compound **3e** (97% yield). ^{1}H NMR (400 MHz, $CDCl_3$) δ 7.93 – 7.63 (m, 4H), 7.43 (s, 1H), 7.35 – 7.04 (m, 5H), 5.64 (d, *J* = 5.2 Hz, 1H), 5.13 – 4.87 (m, 3H), 4.02 – 3.75 (m, 4H), 3.76 – 3.35 (m, 4H), 3.29 – 2.95 (m, 4H), 2.96 – 2.58 (m, 4H), 1.93 – 1.81 (m, 1H), 1.69 (d, *J* = 6.7 Hz, 3H), 0.90 (dd, *J* = 15.4, 6.5 Hz, 6H). ^{13}C NMR (125 MHz, $CDCl_3$) δ 166.7, 157.4,

155.4, 137.7, 135.9, 131.8, 129.2, 128.8, 128.5, 128.0, 127.9, 126.5, 124.5, 124.0, 109.2, 78.5, 73.4, 70.9, 69.8, 69.5, 63.7, 58.5, 55.8, 53.4, 46.4, 35.8, 29.6, 27.1, 25.7, 21.3, 20.0, 19.9. LRMS-ESI (*m/z*): 644.4 $[M+H]^+$, 666.4 $[M+Na]^+$. HPLC analysis: Chiralpak IC column, 75% isopropanol in *n*-hexane, flow = 0.8 mL/min, t = 24 °C, λ = 254 nm, rt = 13.8 min, *dr* > 99:1.

(3*R*,3a*S*,6a*R*)-Hexahydrofuro[2,3-*b*]furan-3-yl ((2*S*,3*R*)-3-hydroxy-4-((4-(2-((*S*)-1-hydroxyethyl)oxazol-5-yl)-*N*-isobutylphenyl)sulfonamido)-1-phenylbutan-2-yl)carbamate (3l):

Compound **3l** was obtained from compound **3j** following the same procedure described for compound **3f** (95% yield). ^{1}H NMR (400 MHz, $CDCl_3$) δ 7.90 – 7.71 (m, 4H), 7.44 (s, 1H), 7.31 – 7.10 (m, 5H), 5.64 (d, *J* = 5.2 Hz, 1H), 5.07 – 4.98 (m, 2H), 4.88 – 4.83 (m, 1H), 3.98 – 3.80 (m, 4H), 3.71 – 3.52 (m, 4H), 3.10 – 2.88 (m, 4H), 2.85 – 2.72 (m, 4H), 1.87 – 1.79 (m, 1H), 1.68 (d, *J* = 6.7 Hz, 3H), 0.91 (dd, *J* = 15.3, 6.5 Hz, 6H). ^{13}C NMR (125 MHz, $CDCl_3$) δ 166.7, 157.6, 155.4, 137.4, 135.8, 131.7, 129.2, 128.8, 128.5, 128.0, 127.4, 126.5, 124.5, 109.3, 78.5, 73.0, 70.8, 69.8, 69.5, 63.7, 58.4, 53.4, 46.5, 35.8, 29.5, 27.1, 24.8, 21.2, 20.0, 19.8. LRMS-ESI (*m/z*): 644.4 $[M+H]^+$, 666.3 $[M+Na]^+$. HPLC analysis: Chiralpak IC column, 75% isopropanol in *n*-hexane, flow = 0.8 mL/min, t = 24 °C, λ = 254 nm, rt = 11.2 min, *dr* > 99:1.

Determination of X-ray structure of HIV-1 protease and inhibitor 3g complex: The optimized HIV-1 protease was expressed and purified as described.[35] The protease-inhibitor complex was crystallized by the hanging drop vapor diffusion method with well solutions of 1.3 M NaCl, 0.1M sodium acetate buffer (pH 5.5). Diffraction data were collected on a single crystal cooled to 90 K at SER-CAT (22-ID beamline), Advanced Photon Source, Argonne National Lab (Chicago, USA) with X-ray wavelength of 0.8 Å, and processed by HKL-2000[36] with an Rmerge of 6.2%. Using the isomorphous structure[37] the crystal structure was solved by PHASER[38] in the CCP4i Suite[39-41] and refined in SHELX-97[42-44] with 1.3 Å resolution data. COOT[43,45] was used for manual modification of the atomic structure. PRODRG-2[46] was used to construct the inhibitor and the restraints for refinement. Alternative conformations were modeled, anisotropic atomic displacement parameters (B factors) were applied for all atoms including solvent molecules, and hydrogen atoms were added in the final round of refinement. The final refined solvent structure comprised two Na^+ ion, four Cl^- ions, and 234 water molecules. The crystallographic statistics are listed in a Table in the supporting information. The coordinates and structure factors of the PR with GRL-05311A structure have been deposited in Protein Data Bank[47] with PDB ID: 6B4N.

Acknowledgements

This research was supported by the National Institutes of Health (Grant GM53386, AKG and Grant GM62920, ITW). This work was also supported by the Intramural Research Program of the Center for Cancer Research, National Cancer Institute, National Institutes of Health, and in part by a Grant-in-Aid for Scientific Research (Priority Areas) from the Ministry of Education, Culture, Sports, Science, and Technology of Japan (Monbu Kagakusho), a Grant for Promotion of AIDS Research from the Ministry of Health, Welfare, and Labor of Japan, and the Grant to the Cooperative Research Project on Clinical and Epidemiological Studies of Emerging and Reemerging Infectious Diseases (Renkei Jigyo) of Monbu-Kagakusho. The authors would like to thank the Purdue University Center for Cancer Research, which supports the shared NMR and mass spectrometry facilities.

Keywords: HIV-1 protease inhibitors • P2' ligand • Drug resistance • Pharmacokinetics • Structure-based design and synthesis

References:

[1] NAIDS/WHO, AIDS Epidemic Update December 2006.
[2] W. C. Greene, *Eur. J. Immunol.* **2007**, *37*, S94-S102.
[3] K. A. Sepkowitz, *N. Engl. J. Med.* **2001**, *344*, 1764-1772.
[4] A. Edmonds, M. Yotebieng, J. Lusiama, Y. Matumona, F. Kitetele, S. Napravnik, S. R. Cole, A. Van Rie, F. Behets, *PLoS Med.* **2011**, 8e1001044.
[5] M. S. Cohen, Y. Q. Chen, M. McCauley, *N. Engl. J. Med.* **2011**, *365*, 493-505.
[6] C. W. Diffenbach, A. S. Fauci, *Ann Intern Med.* **2011**, *154*, 766-771.
[7] G. Maartens, C. Celum, S. Lewin, *Lancet*. **2014**, *384*, 258-271.
[8] T. Cihlar, M. Fordyce, *M. Curr. Opin. Virol.* **2016**, *18*, 50-56.
[9] K. Patel, M. A. Hernán, P. L. Williams, J. D. Seeger, K. McIntosh, R. B. Van Dyke, G. R. Seage III, *Clin. Infect. Dis.* **2008**, *46*, 507-515.
[10] R. Gupta, A. Hill, A. W. Sawyer, D. Pillay, *Clin. Infect. Dis.* **2008**, *47*, 712-722.
[11] S. Hue, R. J. Gifford, D. Dunn, E. Fernhill, D. Pillay, *J. Virol.* **2009**, *83*, 2645-2654.
[12] A. K. Ghosh, H. L. Osswald, G. Prato, *J. Med. Chem.* **2016**, *59*, 5172-208.
[13] A. K. Ghosh, B. Chapsal, H. Mitsuya, Darunavir, a New PI with Dual Mechanism: From a Novel Drug Design Concept to New Hope Against Drug-Resistant HIV. In: Aspartic Acid Proteases as Therapeutic Targets., Wiley-VCH Verlag GmbH & Co. KGaA: Weinheim, **2010**, 205-243.
[14] A. K. Ghosh, B. D. Chapsal, I. T. Weber, H. Mitsuya, *Acc. Chem. Res.* **2008**, *41*, 78-86.
[15] A. K. Ghosh, B. D. Chapsal Design of the anti-HIV protease inhibitor darunavir. In 'From Introduction to Biological and Small Molecule Drug Research and Development' Ed. Ganellin, C. R.; Roberts, S. M.; Jefferis, R. **2013**, 355-384.
[16] A. K. Ghosh, Z. L. Dawson, H. Mitsuya, *Bioorg. Med. Chem.* **2007**, *15*, 756-7580.
[17] Y. Koh, H. Nakata, K. Maeda, H. Ogata, G. Bilcer, T. Devasamudram, J. F. Kincaid, P. Boross, Y.-F. Wang, Y. Tie, P. Volarath, L. Gaddis, R. W. Harrison, I. T. Weber, A. K. Ghosh, H. Mitsuya, *Antimicrob. Agents Chemother.* **2003**, *47*, 3123-3129.
[18] D. L. N. G. Surleraux, A. Tahri, W. G. Verschueren, G. M. E. Pille, H. A. de Kock, T. H. M. Jonckers, A. Peeters, S. De Meyer, H. Azijn, R. Pauwels, M.-P. de Bethune, N. M. King, M. Prabu-Jeyabalan, C. A. Schiffer, P. B. T. P. Wigerinck, *J. Med. Chem.* **2005**, *48*, 1813-1822.
[19] On June 23, 2006, FDA approves Darunavir for HIV treatment-experienced patients, and in December 13, 2008 for treatment-naïve patients and pediatrics. Available at http://www.accessdata.fda.gov/scripts/cder/drugsatfda/index.cfm, (accessed September 2017).
[20] Y. Tie, P. I. Boross, Y.-F. Wang, L. Gaddis, A. K. Hussian, S. Leshchenko, A. K. Ghosh, J. M. Louis, R. W. Harrison, I. T. Weber, *J. Mol. Biol.* **2004**, *338*, 341-352.
[21] A. K. Ghosh, D. D. Anderson, I. T. Weber, H. Mitsuya, *Angew. Chem. Int. Ed.* **2012**, *51*, 1778-1802.
[22] R. S. Yedidi, K. Maeda, W. S. Fyvie, et al. *Antimicrob. Agents Chemother.* **2013**, *57*, 4920-4927.

[23] A. Y. Kovalevsky, Y. Tie, F. Liu, P. I. Boross, Y.-F. Wang, S. Leshchenko, A. K. Ghosh, R. W. Harrison, I. T. Weber, *J. Med. Chem.* **2006**, *49*, 1379-1387.

[24] R. S. Yedidi, H. Garimella, M. Aoki, H. Aoki-Ogata, D. V. Desai, S. B. Chang, D. A. Davis, W. S. Fyvie, J. D. Kaufman, D. W. Smith, D. Das, P. T. Wingfield, K. Maeda, A. K. Ghosh, H. Mitsuya, *Antimicrob. Agents Chemother*. **2014**, *58*, 3679-3688.

[25] A. K. Ghosh, P. R. Sridhar, S. Leshchenko, A. K. Hussain, J. Li, A. Y. Kovalevsky, D. E. Walters, J. E. Wedekind, V. Grum-Tokars, D. Das, Y. Koh, K. Maeda, H. Gatanaga, I. T. Weber, H. Mitsuya, *J. Med. Chem.*, **2006**, *49*, 5252-5261.

[26] A. K. Ghosh, P. R. Sridhar, N. Kumaragurubaran, Y. Koh, I. T. Weber, H. Mitsuya, *ChemMedChem*, **2006**, *1*, 939-950.

[27] F. Couty, O. David, B. Larmanjat, J. Marrot, *J. Org. Chem.* **2007**, *3*, 1058-1061.

[28] A. Fujii, S. Hashiguchi, N.Uematsu, T. Ikariya, R. Noyori, *J. Am. Chem. Soc.*, **1996**, *118*, 2521–2522.

[29] A. J. Phillips, Y. Uto, P. Wipf, M. J. Reno, D. R. Williams, *Org. Lett.* **2000**, *2*, 1165-1168.

[30] A. M. Van Leusen, B. E. Hoogenboom, H. Siderius, *Tetrahedron Lett*. **1972**, *23*, 2369-2372.

[31] D. J. Pippel, C. M. Mapes, N. S. Mani, *J. Org. Chem.* **2007**, *72,* 5828-5831.

[32] M. V. Toth, G. R. Marshall, *Int. J. Pept. Protein Res*. **1990**, *36*, 544−550.

[33] Y. Koh, M. Amano, T. Towata, M. Danish, S. Leshchenko-Yashchuk, D. Das, M. Nakayama, Y. Tojo, A. K. Ghosh, H. Mitsuya, *J. Virol*. **2010**, *84*, 11961−11969.

[34] Y. Koh, D. Das, S. Leschenko, H. H. Nakata, Ogata-Aoki, M. Amano, M. Nakayama, A. K. Ghosh, H. Mitsuya, *Antimicrob Agents Chemother*. **2009**, 53, 997-1006.

[35] B. Mahalingam, J. M. Louis, J. Hung, R. W. Harrison, I. T. Weber, *Proteins* **2001**, 43, 455–464.

[36] Z. Otwinowski, W. Minor Processing of X-ray Diffraction Data Collected in Oscillation Mode. Methods in Enzymology, 276: Macromolecular Crystallography, Part A; Carter, C.W., Jr., Sweet, R. M., Eds.; Academic Press: New York, 1997; pp 307-326.

[37] C.-H. Shen, Y.-F. Wang, A. Y. Kovalevsky, R. W. Harrison, I. T. Weber, *Febs J.* **2010**, 277, 3699-3714.

[38] A. J. McCoy, R. W. Grosse-Kunstleve, P. D. Adams, M. D. Winn, L. C. Storoni, R. J. Read, *J. Appl. Crystallogr.* **2007**, 40, 658–674.

[39] M. D. Winn, C. C. Ballard, K. D. Cowtan, et al. *Acta Crystallogr., Sect. D: Biol. Crystallogr.* **2011**, 67, 235-242.

[40] Collaborative Computational Project, Number 4 *Acta Crystallogr., Sect. D: Biol. Crystallogr.,* **1994**, 50, 760-763.

[41] E. Potterton, P. Briggs, M. Turkenburg, E. Dodson, *Acta Crystallogr., Sect. D: Biol. Crystallogr.* **2003**, 59, 1131–1137.

[42] G. M. Sheldrick *Acta Crystallogr., Sect. A: Found. Crystallogr.* **2008**, 64, 112–122.

[43] G. M. Sheldrick, T. R. Schneider, *Methods Enzymol.* **1997**, 277, 319–343.

[44] P. Emsley, B. Lohkamp, W. G. Scott, K. Cowtan, *Acta Crystallogr., Sect. D: Biol. Crystallogr.* **2010**, 66, 486-501.

[45] P. Emsley, K. Cowtan, *Acta Crystallogr., Sect. D: Biol. Crystallogr.* **2004**, 60, 2126–2132.

[46] A. W. Schuettelkopf, D. M. F. van Aalten, *Acta Crystallogr., Sect. D: Biol. Crystallogr.* **2004**, 60, 1355–1363.

[47] H. M. Berman, J. Westbrook, Z. Feng, G. Gilliland, T. N. Bhat, H. Weissig, I. N. Shindyalov, P. E. Bourne, *Nucleic Acids Res.* **2000**, 28, 235–242.

Received: ((will be filled in by the editorial staff))

10.1002/cmdc.201700614

Entry for the Table of Contents

Insert graphic for Table of Contents here.

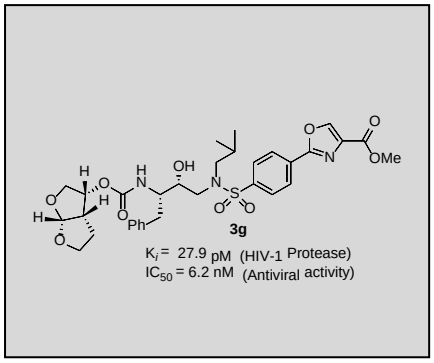

We report structure-based design, synthesis, biological evaluation and X-ray structural studies of a series of highly potent HIV-1 protease inhibitors containing novel P2' –ligands to interact with active site residues.